

Cobbold, C. A., Lutscher, F. and Yurk, B. (2022) Bridging the scale gap: predicting large-scale population dynamics from small-scale variation in strongly heterogeneous landscapes. *Methods in Ecology and Evolution*, 13(4), pp. 866-879. (doi: [10.1111/2041-210X.13799](https://doi.org/10.1111/2041-210X.13799))

The material cannot be used for any other purpose without further permission of the publisher and is for private use only.

There may be differences between this version and the published version. You are advised to consult the publisher's version if you wish to cite from it.

This is the peer reviewed version of the following article:

Cobbold, C. A., Lutscher, F. and Yurk, B. (2022) Bridging the scale gap: predicting large-scale population dynamics from small-scale variation in strongly heterogeneous landscapes. *Methods in Ecology and Evolution*, 13(4), pp. 866-879, which has been published in final form at: [10.1111/2041-210X.13799](https://doi.org/10.1111/2041-210X.13799)

This article may be used for non-commercial purposes in accordance with [Wiley Terms and Conditions for Self-Archiving](#).

<https://eprints.gla.ac.uk/259569/>

Deposited on: 26 November 2021

Enlighten – Research publications by members of the University of
Glasgow

<http://eprints.gla.ac.uk>

1 Bridging the scale gap: predicting large-scale
2 population dynamics from small-scale variation in
3 strongly heterogeneous landscapes

4 Christina A. Cobbold^{*,1,2}, Frithjof Lutscher³, & Brian Yurk⁴

5 November 25, 2021

6 ¹ *School of Mathematics and Statistics, University of Glasgow, Glasgow, G12 8QW, United*
7 *Kingdom*

8 ² *Boyd Orr Centre for Population and Ecosystem Health, University of Glasgow, Glasgow, G12*
9 *8QW, United Kingdom.*

10 ³ *Department of Mathematics and Statistics, and Department of Biology, University of Ottawa,*
11 *Ottawa, ON, K1N 6N5, Canada.*

12 ⁴ *Department of Mathematics and Statistics, Hope College, Holland, Michigan 49422-9000,*
13 *USA.*

14
15 *Corresponding author: christina.cobbold@glasgow.ac.uk

16
17 **Running Headline** Bridging the scale gap

18
19 **Keywords** dynamic level, habitat fragmentation, heterogeneity, homogenization, multi-
20 scale, reaction-diffusion equation, residence index, wildlife-habitat modeling,

Abstract

1. Often, ecologists are challenged with a mismatch of scales: how do we up-scale from local variation and available data to landscape-level models and predictions?
2. We present a general recipe for coarse-graining from local to landscape-scale reaction-diffusion equations when spatial heterogeneity is small in extent compared to dispersal of organisms. Our homogenization approach uses the fundamental ecological concepts of Turchin's *residence index* and Skellam's *dynamic level*.
3. Our approach opens avenues to new ecological theory that connects different scales, which we illustrate using predator-prey interactions. It also presents opportunities for using the increasingly available small-scale data for landscape-level predictions, such as range expansion rates.
4. We find several unexpected nonlinear relationships between the movement behavior on the local level and the spatially implicit and explicit outcomes at the landscape-level, e.g., predator spread rate may increase *or* decrease when predators move faster locally. Our method provides a mechanistic link for population dynamics and data integration across spatial and temporal scales, addressing a fundamental goal of landscape ecology.

1 Introduction

Ecologists are often challenged by complex scale relationships: we want to understand and predict population dynamics on large spatial and temporal scales, but we can typically only measure and observe processes on small scales. Methods exist to obtain local population growth and movement models from observational data (e.g., Turchin (1998)). Theory exists to calculate, say, spread rates and persistence conditions from homogeneous

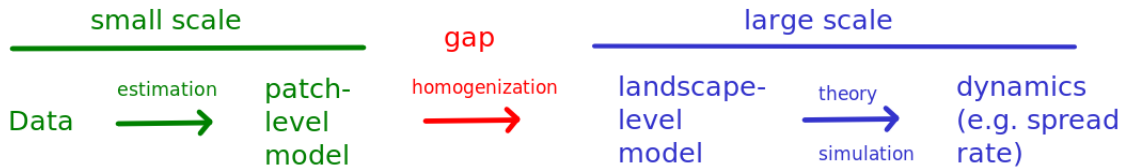


Figure 1: The gap between available small-scale observation (green, left) and desired large-scale prediction (blue, right). Data are available on the small scale and methods exist for estimating parameters for patch-level models (Turchin, 1998). Theory is in place and simulation is feasible to obtain desired outcomes from landscape-level models (Fagan *et al.*, 2002). We show here that homogenization theory helps bridge the gap; see also Garlick *et al.* (2011, 2014).

47 landscape-level models (e.g., Fagan *et al.* (2002)). How to obtain landscape-level models
 48 from habitat-level information is the gap that we bridge here (Figure 1). Our approach is
 49 based on homogenization, a mathematical theory of coarse-graining or weighted averaging,
 50 with weights that emerge from the theory. It applies when individuals, over their lifetimes,
 51 experience several different habitat types that affect their movement behaviors and vital
 52 rates. Our formulas give precise relationships for how to include small-scale variation
 53 into landscape-scale models. Our method can be used to develop new understanding of
 54 mechanisms that drive large-scale population outcomes, and also to connect increasingly
 55 available small-scale experimental and observational data to large-scale predictions (e.g.,
 56 range expansion speed) that can inform landscape management.

57 In a review of multi-scale empirical studies, Wheatley and Johnson (2009) find little
 58 consistency in the choice of observational scales in experiments, which makes cross-scale
 59 results difficult to compare and generalize. Whenever empirical data of ecological in-
 60 teractions are collected, movement and habitat heterogeneity must be taken into account
 61 through appropriate scaling. How to do this, is the general question of upscaling or coarse-
 62 graining. It is an old tenet, following for example from Jensen’s inequality, that one should
 63 “not average the data, but average the model.” Researchers have developed mean field,
 64 pair approximation and moment methods (Metz, 2000), scale transition theory (Chesson,
 65 1998; Melbourne and Chesson, 2006; Chesson, 2012), used dimensional analysis (Englund

66 and Cooper, 2003) and statistical approaches (Inouye, 2005), or considered experimental
67 design (Hewitt *et al.*, 2007) to address this. Such methods were reviewed in a dedicated
68 journal issue (Morozov and Poggiale, 2012). All these approaches make several somewhat
69 similar assumptions of scale separation, for example that interactions are local or that
70 individuals experience the full range of landscape variation during their lifetime (Getz
71 *et al.*, 2018; Morozov and Poggiale, 2012). They obtain results on an aggregate level,
72 such as overall population growth rate, that contains space only implicitly. Our method
73 makes similar assumptions (see box in Figure 2) but retains a spatially explicit dynamic
74 model, from which one can then derive quantities such as overall population growth rate
75 (as in previous models) or spatial spread rate (that cannot be obtained from previous
76 approaches).

77 Recent models of individual movement and population growth in strongly heteroge-
78 neous (“patchy”) landscapes and their applications to invasion and conservation ecology
79 show certain surprising effects, which could easily have been missed with aggregate models
80 that do not incorporate the same level of small-scale detail. Maciel and Lutscher (2013)
81 studied population dynamics in patchy landscapes with reaction–diffusion equations that
82 included individual movement behavior at patch boundaries and patch preferences. This
83 information is available from field studies for many species (Crone and Schultz, 2008;
84 Reeve *et al.*, 2008). Applying this modeling framework, Lutscher and Musgrave (2017)
85 showed that reducing host availability could have the unintended consequence of speeding
86 up the range expansion of a forest insect pest. Similarly, Crone *et al.* (2019) demonstrated
87 the importance of relatively small fractions of high-quality habitat for conservation and
88 range expansion of species at risk.

89 Including large amounts of small-scale data into population models increases model
90 complexity and inhibits explicit analysis. Even numerical simulations often require ad-
91 vanced techniques such as adaptive mesh refinement (Gilbert *et al.*, 2017). Our method is
92 based on homogenization analysis of multiscale models (Pavliotis and Stuart, 2008). The

93 underlying idea is that if individuals encounter many habitat types during their lifetime,
94 then their lifetime dynamics should be approximated reasonably well by an appropriately
95 weighted average of the conditions encountered in these habitats. The goal is to obtain the
96 correct averages that lead to a homogeneous landscape-level model with (approximately)
97 the same properties as the model that includes all the detailed small-scale information.

98 Some applications of homogenization to spatial spread models exist, e.g., Reid’s para-
99 dox (Powell and Zimmermann, 2004), or chronic wasting disease (Garlick *et al.*, 2014). For
100 sessile organisms (e.g., plants), the requirement that an individual experiences different
101 habitat types can be replaced by its offspring (e.g., seeds) covering many different habitat
102 types; see Neupane and Powell (2015) for tree migration mitigated by birds, or Duncan
103 *et al.* (2017) for invasive plants. In all these cases, the scale of landscape variation (y)
104 was small compared to the extent (x) of the phenomenon, so that individuals encounter
105 many different habitat types during their life time. In fact, different scales, expressed as
106 the ratio $\varepsilon = y/x$, arise in many ecological systems (Table 1). If they do, homogenization
107 theory helps reduce complex, spatially heterogeneous equations to simpler, spatially ho-
108 mogeneous equations that nonetheless approximate the behavior of the complex equations
109 very well (Pavliotis and Stuart, 2008). The parameters of the homogenized model encode
110 the patch-scale variation as appropriate multiscale averages.

111 In patchy landscapes, the abrupt change in environmental conditions across patch
112 edges prohibits us from applying classical homogenization theory directly. Previous ap-
113 plications were somewhat case specific, but Yurk and Cobbold (2018) presented the first
114 rigorous treatment for a single-species model. Applications of their theory to competition
115 systems (Maciel and Lutscher, 2018) and stage-structured populations (Alqawasmeh and
116 Lutscher, 2019) demonstrated the usefulness of homogenization theory and reiterated the
117 importance of including small-scale processes in large-scale models. The approach in Yurk
118 and Cobbold (2018) is highly technical, but the mathematical theory has now matured so
119 that it connects to long-standing concepts from ecological theory and can be consistently

120 used and applied to multi-species systems.

121 We present our general homogenization method for transforming a multi-patch reaction-
122 diffusion model with spatial variation on the small scale into a landscape model with ap-
123 propriately averaged coefficients. The method enables the development of ecological the-
124 ory that explains landscape-level population outcomes in terms of habitat-level quantities,
125 and it allows the use of local data in landscape models to predict large-scale outcomes such
126 as spatial spread rates. We focus on the case of two interacting species and two habitat
127 types, though it is straightforward to extend the method to additional species and habi-
128 tats. We illustrate the utility of the method by applying it to predator-prey interactions.
129 We uncover new connections between the large-scale properties of the system, e.g., an
130 effective landscape-scale functional response, and the movement behavior at the habitat
131 level. We present our method for simplified one-dimensional habitats where two patch
132 types alternate periodically in space. This setting may seem somewhat limiting for ap-
133 plications, but it provides a first important step towards including fine-scale information
134 into large-scale prediction. Moreover, the interpretation of our formulas does not require
135 the periodicity assumption, and we speculate that they apply more generally, although
136 the mathematical theory on this matter is still being developed. The extension to two
137 spatial dimensions seems more challenging; we return to this question in the discussion.
138 The one-dimensional theory is best suited for applications to spatial spread, which is our
139 focus here. We summarize the key assumptions of our method in the box in Figure 2.

140 **2 Methods**

141 Our method takes a multi-patch reaction-diffusion model with spatial variation on the
142 small-scale into a landscape model with appropriately averaged coefficients on the large-
143 scale. The mathematical aspects of homogenization theory are quite technical (Pavliotis
144 and Stuart, 2008); see Supplementary Material. The underlying ideas, however, are quite
145 intuitive: If the environment of an organism changes rapidly in time, the growth of

Example	Landscape scale (x)	Habitat scale (y)	Slow time scale (t)	Fast time scale (τ)	ε
Spread of chronic wasting disease in deer ¹	3km (daily deer movement)	30 meters (landscape classification)	years (time scale of infection)	days	0.01
Seed dispersal by animals ²	100's meters (plant migration)	~ 2 meters (seed caching)	100's years	year	0.01
Spread of Mountain Pine beetle ³	kilometers (dispersal distance)	hectare (forest composition)	year (generation time)	hours/day (beetle dispersal)	0.1
Marine green turtle homing navigation ⁴	20 kilometers (daily movement)	1 kilometer (flow field changes)	1 month (navigation time)	day	0.1

Table 1: Example study systems where habitat averaging is applicable: ε is the ratio of habitat (y) to landscape-scale (x). ¹ Garlick *et al.* (2011). ² Powell and Zimmermann (2004). ³ Powell and Bentz (2014). ⁴ Painter and Hillen (2015).

146 the organism is well described by some appropriately weighted temporal average of the
147 environmental conditions (Hastings, 2012). If, instead, an organism moves through a
148 temporally constant but spatially varying landscape of many patches, it will encounter
149 the conditions on the different patches as temporal variation. As in the temporal case,
150 the organisms' growth should then be determined by a suitable average of this spatial
151 variation with weights that indicate how much time the organism spends in the different
152 patches.

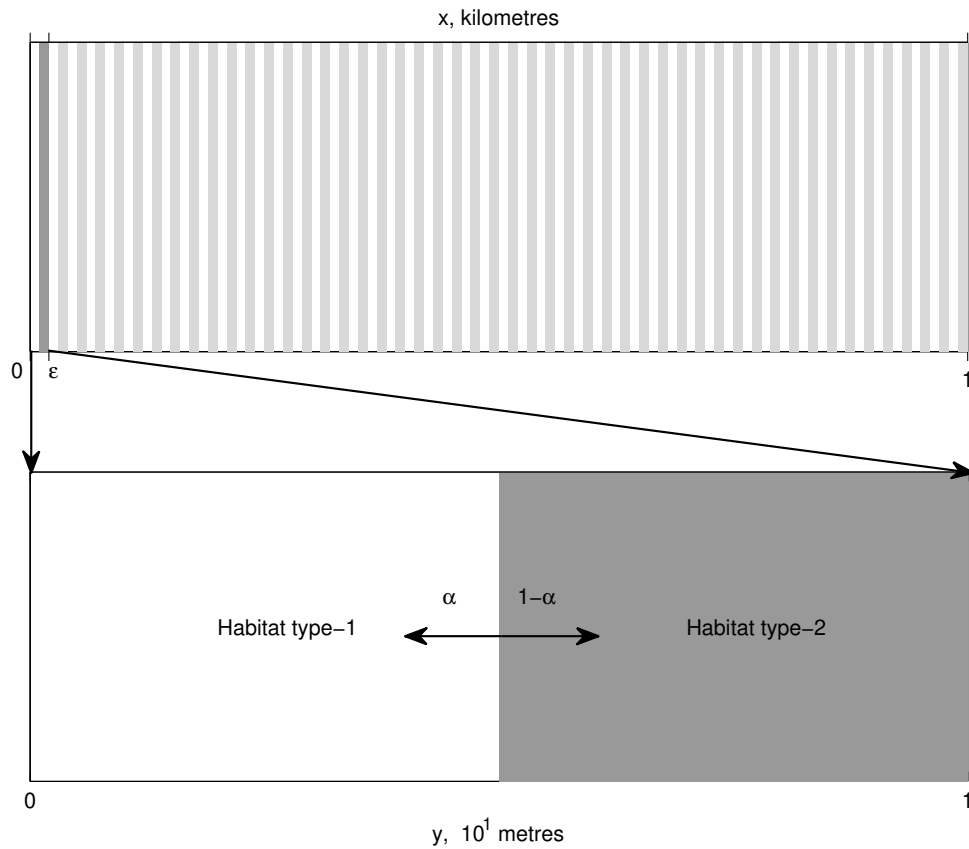
153 Bridging the scale gap consists of three steps. First, one identifies the appropriate
154 spatial and temporal scales and formulates a reaction-diffusion model for demography
155 and movement within and between small-scale patches. Second, one applies our method
156 of homogenization to derive the large-scale model. Because of scale separation, habitat-
157 level demography is slow compared to movement within and between adjacent patches,
158 so that appropriately averaged population growth acts on locally equilibrated movement
159 dynamics. The resulting model and formulas for the averaged coefficients are given in
160 Table 2. Third, one analyzes the landscape-scale model according to the question at
161 hand, e.g., to derive population persistence conditions or spread rates.

162 2.1 Step 1: Defining spatial and temporal scales

163 We choose the spatial and temporal scales according to the scientific questions considered.
164 For example, to study the spread of an organism on a scale of kilometres in a landscape
165 consisting of several habitat types, each of which extends on the order of 100 metres, we
166 naturally have (i) the landscape-scale measured in kilometres and (ii) the habitat-scale
167 measured in 100s of metres. Central to our approach is the assumption that the habitat-
168 scale is (much) smaller than the landscape-scale. We denote by ε the ratio of the two
169 scales ($\varepsilon = 0.1$ in the example). The density of the organism scales accordingly: if there
170 are U organisms per kilometre on the landscape-scale then there are $u = \varepsilon U$ organisms
171 per 100 metres on the habitat-scale.

172 Our next central assumption is that organisms, through dispersal, encounter several
173 habitat types over their lifetime, and that the time they spend in any one habitat is
174 relatively short. Hence, we also have two temporal scales. We expect that the phenomenon
175 on the landscape-scale over large times is sufficiently well described by an appropriate
176 average of the processes on the habitat-scale over short times. We also expect that the
177 times spent in each habitat appear as weights in this average.

178 To define the two temporal scales, we consider the analogy of a movie. Suppose we
179 watch a movie of a biological invasion, where the width of the screen corresponds to several
180 kilometers (landscape) and time corresponds to years. To observe the same invasion on
181 the habitat-scale, we would “zoom in” so that the screen corresponds to several hundred
182 metres (habitat). We specify a magnification factor, such that y 100s of metres on the
183 habitat-scale is $x = \varepsilon y$ kilometres on the landscape-scale (Figure 2). Simultaneously, we
184 would need to slow down the movie or else the invasion would pass through the screen
185 too quickly. Accordingly, we define a scaling factor ($\hat{\varepsilon}$) that relates τ units of the short
186 time to $t = \hat{\varepsilon}\tau$ time units on the long time scale, which is given by the phenomenon that
187 we study (e.g., in years). The scaling factor for time is determined by the movement
188 model that we use. For a diffusion process, we choose the shorter time scale such that



Key assumptions in our work

1. Habitat varies on a much smaller scale than the landscape-scale.
2. Organisms encounter several habitat types over the course of their lifetime and spend relatively little time in any one habitat.
3. On the habitat-scale, the effects of intra- and interspecific interactions on demography are small compared to movement.
4. Movement can be described by a diffusion process (can be generalized).
5. The landscape is periodic (can be generalized).
6. The landscapes is one-dimensional (can be generalized).

Figure 2: Illustration of spatial scales: landscape (top panel) and habitat (lower panel). Individuals at a patch interface move to habitat 1 with probability α and to habitat 2 with probability $1 - \alpha$. The first three key assumptions are essential for applying homogenization theory. Assumptions 4–6 are used here to obtain explicit formulas but can be generalized. All assumptions and their implied limitations are examined in more detail in the discussion.

189 the magnitude of the mean squared displacement per unit time (MSD) of the organism is
 190 the same when viewed on the landscape- or the habitat-scale:

$$\text{MSD} = \frac{\text{distance}^2}{\text{time}} = \frac{\overbrace{\langle y^2 \rangle}^{\text{Magnitude of habitat-scale MSD}}}{\tau} = \frac{\overbrace{\langle x^2 \rangle}^{\text{Magnitude of landscape-scale MSD}}}{t}. \quad (1)$$

191 Substituting $x = \varepsilon y$ and $t = \hat{\varepsilon} \tau$ to find $\hat{\varepsilon}$, the scaling factor for time is $\hat{\varepsilon} = \varepsilon^2$. For the
 192 example where the landscape is measured in kilometres and the invasion is observed over
 193 years, a habitat-scale of 100 metres gives $\varepsilon = 0.1$ and $\hat{\varepsilon} = 0.01$. Thus, our short time scale
 194 is 0.01×1 year, roughly half a week. If we choose transport instead of diffusion models
 195 for movement, we obtain a different temporal scaling (Lutscher and Hillen, 2021).

196 The examples in Table 1 satisfy our key assumptions (see Figure 2). In practice, the
 197 method works surprisingly well even when the difference in spatial scales is not as large
 198 and/or if organisms encounter only few habitat types over their lifetime. Simulations
 199 show a very good approximation of the full model by the homogenization (Garlick *et al.*,
 200 2011; Duncan *et al.*, 2017; Yurk and Cobbold, 2018).

201 **2.2 Step 2: Patch-level reaction-diffusion equations and land-** 202 **scape equations**

203 Our idealized landscape consists of periodically alternating patches of two different habitat
 204 types (Shigesada *et al.*, 1986), whose spatial extent is much smaller than the scale of the
 205 study question (Figure 2). We formulate reaction-diffusion equations for two interacting
 206 populations on each habitat patch and connect these via interface conditions that describe
 207 individual movement behavior at patch boundaries. We denote by y (x) the spatial
 208 coordinate on a habitat patch (landscape) and by τ (t) the fast (slow) time-scale. These
 209 quantities are related by $x = \varepsilon y$ and $\tau = \varepsilon^2 t$ (see above). The length of a habitat patch
 210 of type i , measured on the habitat-scale is ℓ_i , such that the period is $\ell_1 + \ell_2 = 1$. On

211 the landscape-scale, the period is ε . We let $u(y, \tau)$ and $v(y, \tau)$ denote the density of the
 212 two populations on the habitat-scale. The reaction-diffusion equations governing their
 213 dynamics are

$$\text{Habitat level dynamics} \left\{ \begin{array}{l} \frac{\partial u}{\partial \tau} = D_i^u \frac{\partial^2 u}{\partial y^2} + \varepsilon^2 f_i(u, v), \\ \frac{\partial v}{\partial \tau} = D_i^v \frac{\partial^2 v}{\partial y^2} + \varepsilon^2 g_i(u, v), \end{array} \right. \quad (2)$$

214 where D_i^u (D_i^v) denote the diffusion coefficients of population u (v) on type- i habitat.
 215 Functions f_i and g_i denote the net growth of u and v on habitat type i , respectively.
 216 The factor ε^2 indicates that demography on the habitat-scale is slow compared to the
 217 landscape-scale. At a boundary between two habitat types, individuals of population u
 218 (v) choose to move to habitat type 1 with probability α^u (α^v) and to habitat type 2 with
 219 probability $1 - \alpha^u$ ($1 - \alpha^v$); see Supplementary Material S.1 for details.

220 We define $U(x, t)$ and $V(x, t)$ as the respective population densities at the landscape-
 221 scale, averaged over habitat types. Strictly speaking, U and V are approximations to this
 222 spatial average. Yurk and Cobbold (2018) showed, by numerical simulation, that they are
 223 highly accurate under the assumptions in Figure 2. The equations that these variables
 224 satisfy are given in Table 2 and discussed in the next section. Their derivation can be
 225 found in Supplementary Material S.1.

226 3 Results

227 The population densities on the landscape-scale, averaged over one period at the habitat-
 228 scale, satisfy the habitat-averaged landscape equations (HALE), Table 2, equations (3).
 229 At this level, the equations are homogeneous, but the diffusion coefficients and the growth
 230 functions are appropriate averages, indicated by $\hat{}$, of the small-scale heterogeneity (also
 231 in Table 2). We give a detailed discussion novel interpretations in terms of the classic

Habitat-averaged landscape equations (HALE)

$$\text{Landscape level dynamics} \begin{cases} \frac{\partial U}{\partial t} = \hat{D}^u \frac{\partial U}{\partial x^2} + \hat{f}(U, V), \\ \frac{\partial V}{\partial t} = \hat{D}^v \frac{\partial V}{\partial x^2} + \hat{g}(U, V), \end{cases} \quad (3)$$

Here $\hat{f}(U, V)$ is the landscape-scale growth rate for population U ,

$$\hat{f}(U, V) = \frac{\varepsilon^{-1} f_1 \left(\frac{\rho_1^u}{\langle \rho^u \rangle} \varepsilon U, \frac{\rho_1^v}{\langle \rho^v \rangle} \varepsilon V \right) \ell_1 + \varepsilon^{-1} f_2 \left(\frac{\rho_2^u}{\langle \rho^u \rangle} \varepsilon U, \frac{\rho_2^v}{\langle \rho^v \rangle} \varepsilon V \right) \ell_2}{\ell_1 + \ell_2}. \quad (4)$$

The formula for \hat{g} is analogous. The landscape-level diffusion coefficient for U is

$$\hat{D}^u = \langle \alpha^u \rangle^{-1} \langle \rho^u \rangle^{-1} = \left(\frac{(1 - \alpha^u) \ell_1 + \alpha^u \ell_2}{\ell_1 + \ell_2} \right)^{-1} \left(\frac{\rho_1^u \ell_1 + \rho_2^u \ell_2}{\ell_1 + \ell_2} \right)^{-1}, \quad (5)$$

and similar for \hat{D}^v , where ρ_i^u are the habitat residence indices for U :

$$\rho_1^u = \frac{1}{D_1^u (1 - \alpha^u)} \quad \text{and} \quad \rho_2^u = \frac{1}{D_2^u \alpha^u}. \quad (6)$$

We denote by $\langle \cdot \rangle$ the average of a function over one spatial period. The average residence index is then

$$\langle \rho^u \rangle = \frac{\rho_1^u \ell_1 + \rho_2^u \ell_2}{\ell_1 + \ell_2}, \quad (7)$$

and similar for $\langle \rho^v \rangle$.

Table 2: Landscape-scale equations that arise from the homogenization process. The formulas show how the landscape-level parameters and functions are obtained from their habitat-level counterparts.

232 ecological concepts of residence index (Turchin, 1998) and dynamic level (Skellam, 1973).
233 The averaged demography generally differs quantitatively and qualitatively from the local
234 demography (section 3.3).

235 **3.1 Connecting movement to residence indices**

236 Residence indices naturally appears as weights in the averages in Table 2 because of
237 their relation to the time an individual spends in each patch. Turchin (1998) defines
238 the *residence index* at any point in space as a quantity proportional to the steady-state
239 population density in a pure movement model (i.e. without growth). It can be measured
240 empirically (Turchin, 1998). When organisms move via ecological diffusion, the residence
241 index is the inverse of motility (diffusion), so that organism density at steady state is high
242 where motility is low and vice versa. The residence index is therefore a relative measure
243 of the time spent at each location in the absence of births and deaths. Here, residence
244 index is modified by the probability of choosing a certain habitat type, see eq. (6). If, say,
245 an individual preferentially chooses type-1 habitat when it reaches a habitat boundary
246 ($\alpha^u > 1/2$), then the effective leaving rate of type-1 habitat is decreased, and the time
247 spent in type-1 habitat is increased. The reverse is true when preference is for type-2
248 habitat ($\alpha^u < 1/2$).

249 Following Powell and Zimmermann (2004), we use residence index to heuristically
250 derive and explain the expressions for the landscape-level diffusion coefficients (5). We
251 consider a patch of length Δy (with unit length in the perpendicular direction). The
252 residence time in this patch is proportional to (residence index) $\times \Delta y \times 1$, (where the ‘1’
253 stands for the perpendicular direction and carries the units of length). As residence index
254 is defined only up to a constant of proportionality, we scale the residence index by $\langle \alpha^u \rangle$
255 and consider $\rho_i^u \langle \alpha^u \rangle$. This has two useful properties: (i) when there is no patch preference
256 ($\alpha^u = 1/2$), the scaled residence index of habitat i is the inverse of the habitat diffusion
257 coefficient, consistent with Powell and Zimmermann (2004); (ii) the scaled residence index

258 in type-1 (type-2) habitat is an increasing (decreasing) function of α^u , so preference
 259 for habitat 1 increases residence time in habitat 1. Using the scaled residence indices,
 260 residence time in type-1 habitat is proportional to

$$\rho_1^u \langle \alpha^u \rangle \Delta y \times 1 = \frac{1}{D_1^u \frac{1-\alpha^u}{\langle \alpha^u \rangle}} \Delta y, \quad (8)$$

261 and analogously in type-2 habitat. The average residence index in a small region of
 262 landscape is proportional to

$$\frac{\frac{1}{D_1^u \frac{1-\alpha^u}{\langle \alpha^u \rangle}} \ell_1 + \frac{1}{D_2^u \frac{\alpha^u}{\langle \alpha^u \rangle}} \ell_2}{\ell_1 + \ell_2}. \quad (9)$$

263 The inverse of this average (proportional) residence index is exactly the landscape-level
 264 diffusion coefficient in eq. (5), analogous to Powell and Zimmermann (2004), and as it
 265 was for simpler models at the patch level described above (Turchin, 1998).

266 **3.2 Connecting population growth to dynamic level**

267 Dynamic level is related to residence index and appears in the arguments of the growth
 268 functions in eq. (4). In the absence of population growth, Skellam (1973) defines the
 269 *dynamic level* such that individuals diffuse from high to low dynamic level. He uses the
 270 analogy that heat (population) moves in response to differences in temperature (dynamic
 271 level). This is true in materials with jumps in thermal properties, e.g., a hand placed on
 272 a wall. Heat flows if there is a temperature difference between the hand and the wall. At
 273 equilibrium, heat will be discontinuous but temperature will not. Animal populations flow
 274 in response to gradients in dynamic level (from high to low). At equilibrium, the dynamic
 275 level is spatially constant even if the population density is not. In our model, population
 276 density is not spatially constant because of patch preferences and variation in motility
 277 between habitats. We take advantage of the property that dynamic level is spatially con-
 278 stant at steady state in our derivation of the landscape-level equations, and consequently

279 dynamic level appears in the expressions for population growth (Supplementary Material
 280 S.1).

281 Demography is so slow that our model on the habitat-scale can be thought of as a
 282 pure movement model without population growth, allowing us to define the dynamic
 283 level. Turchin (1998) showed that equilibrium population density (u^*) is the dynamic
 284 level multiplied by residence index (ρ), provided movement is not density-dependent. This
 285 allowed him to partition population density into the product of two separate processes,
 286 density-dependence and spatial-dependence (Turchin, 1998):

$$u^*(y) = \overbrace{\rho(y)}^{\text{residence index}} \times \text{const.} = \overbrace{\rho(y)}^{\text{residence index}} \times \overbrace{\frac{\int u^*(y)dy}{\int \rho(y)dy}}^{\text{dynamic level at equilibrium}}. \quad (10)$$

287 The expression for the dynamic level at equilibrium is simply the average density divided
 288 by the average residence index.

289 In our case, the residence index is constant on each habitat patch with values ρ_i^u , and
 290 the average density in a habitat is εU . Hence, the corresponding expression for $u^*(y)$ in
 291 our notation is

$$\overbrace{\rho_i^u}^{\text{residence index}} \times \overbrace{\frac{\varepsilon U}{\langle \rho^u \rangle}}^{\text{dynamic level at equilibrium}}. \quad (11)$$

292 This is exactly the first argument of f_i in eq. (4). Hence, the habitat-level densities that
 293 we consider are precisely the steady-state values of the small-scale movement equations,
 294 expressed in terms of dynamic level and residence index. This could have been expected
 295 since the population changes slowly on the habitat-scale. The landscape-level population
 296 growth functions are then the averages of these habitat-level functions over one spatial
 297 period, converted to density at the landscape-level by dividing by ε .

298 **3.3 Step 3: Analyzing the landscape-scale model, application to**
 299 **predator-prey interactions**

300 Our HALE method gives many insights into how small-scale variation affects large-scale
 301 outcomes, e.g., how functional responses scale from the habitat- to the landscape-level
 302 and how small-scale heterogeneity affects large-scale population persistence and invasion
 303 speed. We illustrate this utility and step 3 of our method by studying the dynamics
 304 of a predator-prey community in a fragmented landscape. We choose a Rosenzweig-
 305 MacArthur model, where the prey grows logistically with growth rate λ and intraspecific
 306 competition strength μ , and is consumed according to functional response ϕ . Prey biomass
 307 is converted into predator biomass linearly with parameter γ . Predators die at rate m . On
 308 the habitat-scale (see (2)), u and v denote the densities of prey and predator, respectively,
 309 with habitat-type dependent functions

$$f_i(u, v) = u(\lambda_i - \mu u) - \phi_i(u)v \quad \text{and} \quad g_i(u, v) = \gamma\phi_i(u)v - mv. \quad (12)$$

310 For simplicity, we assume that γ , μ , and m are independent of habitat type and type-2
 311 habitat always has the lower prey growth rate ($\lambda_2 < \lambda_1$). The non-spatial dynamics are
 312 well known: if λ_i is positive, the prey can grow from low density to carrying capacity
 313 $u^* = \lambda_i/\mu$. If the predator is sufficiently efficient (if $\gamma\phi_i(u^*) - m > 0$), then it can
 314 grow from low density, and there is a positive coexistence state of predator and prey
 315 (Supplementary Material S.4).

316 Applying the HALE framework (Table 2) gives the landscape-scale model

$$\frac{\partial U}{\partial t} = \hat{D}^u \frac{\partial U}{\partial x^2} + (\hat{\lambda} - \hat{\mu}U)U - \hat{\phi}(U)V, \quad \frac{\partial V}{\partial t} = \hat{D}^v \frac{\partial V}{\partial x^2} + \gamma\hat{\phi}(U)V - mV, \quad (13)$$

317 where

$$\hat{\lambda} = \lambda_1 \frac{\rho_1^u}{\langle \rho^u \rangle} \frac{\ell_1}{(\ell_1 + \ell_2)} + \lambda_2 \frac{\rho_2^u}{\langle \rho^u \rangle} \frac{\ell_2}{(\ell_1 + \ell_2)} = \frac{\lambda_1 \rho_1^u \ell_1 + \lambda_2 \rho_2^u \ell_2}{\rho_1^u \ell_1 + \rho_2^u \ell_2} \quad (14)$$

318 and

$$\hat{\mu} = \varepsilon\mu \left[\left(\frac{\rho_1^u}{\langle \rho^u \rangle} \right)^2 \frac{\ell_1}{(\ell_1 + \ell_2)} + \left(\frac{\rho_2^u}{\langle \rho^u \rangle} \right)^2 \frac{\ell_2}{(\ell_1 + \ell_2)} \right] \quad (15)$$

319 are the appropriately averaged low-density growth rate and strength of intraspecific com-
 320 petition. The averaged diffusion coefficients from (5). Clearly, $\hat{\lambda}$ is a weighted average
 321 of the habitat-level growth rates with weights $\rho_i^u \ell_i$, representing the time spent in habi-
 322 tat type i . If the two growth rates are identical ($\lambda_1 = \lambda_2$), then landscape and habitat
 323 growth rate are the same ($\hat{\lambda} = \lambda_1$). Similarly, m does not change between the habitat
 324 and landscape-scale. In contrast, even though μ is constant between the two habitat
 325 types, the effective $\hat{\mu}$ depends on residence times and patch lengths because intraspecific
 326 competition requires interaction between individuals, and therefore depends on how pairs
 327 of individuals spend their time in the different habitats. In particular, $\hat{\mu}$ is the weighted
 328 average of the habitat-level strengths of intraspecific competition, where the weights are
 329 the proportion of time spent in type- i habitat ($\frac{\rho_i^u}{\langle \rho^u \rangle} \cdot \frac{\ell_i}{\ell_1 + \ell_2}$) and the relative density of prey
 330 in type- i habitat ($\frac{\rho_i^u}{\langle \rho^u \rangle}$). The factor of ε in (15) indicates that interactions are rare on the
 331 habitat-scale.

332 We can simplify the expressions by introducing the ratios of the residence indices,
 333 $R^u = \rho_1^u / \rho_2^u$, and patch lengths, $R^\ell = \ell_1 / \ell_2$. We find

$$\hat{\lambda} = \frac{\lambda_1 R^u R^\ell + \lambda_2}{R^u R^\ell + 1} \quad \text{and} \quad \hat{\mu} = \varepsilon\mu \frac{((R^u)^2 R^\ell + 1)(R^\ell + 1)}{(R^u R^\ell + 1)^2}. \quad (16)$$

334 These expressions are particularly useful when relating our models to data since they
 335 require only relative and no absolute measurements.

336 How prey-only dynamics depend on habitat heterogeneity has been studied in detail
 337 by Yurk and Cobbold (2018) and Maciel and Lutscher (2013). Here, we concentrate on
 338 the predator dynamics.

339 **3.3.1 Individual behavior: Functional response**

340 The functional response is a crucial ingredient in modeling the interaction of a predator
 341 and its prey. Scale transition theory shows that the functional response at the landscape
 342 scale can differ in structure from the functional response at the habitat scale (Bergström
 343 *et al.*, 2006; Englund and Leonardsson, 2008; Melbourne and Chesson, 2006). This dif-
 344 ference arises from interaction between spatial variation in population densities and the
 345 nonlinear functional response at the habitat scale (Chesson *et al.*, 2005). We demonstrate
 346 how the landscape-level functional response arises in our homogenization approach and
 347 how that may affect model predictions later. At the habitat level, we choose Holling’s
 348 type II functional response

$$\phi_i(u) = \frac{a_i u}{1 + a_i h_i u} . \quad (17)$$

349 Here, a_i and h_i are the attack rate and the handling time at the habitat level. These two
 350 quantities relate to the graph of $\phi_i(u)$. The slope at zero is $\phi'_i(0) = a_i$ and the asymptote
 351 is $\phi_i(\infty) = 1/h_i$. When prey density is low, predation is limited by the predator’s attack
 352 rate; when prey density is high, it is limited by the handling time.

353 According to formula (4), the functional response on the landscape-level is

$$\widehat{\phi}(U) = \frac{A_1 U}{1 + A_1 H_1 U} + \frac{A_2 U}{1 + A_2 H_2 U} , \quad (18)$$

354 with appropriately scaled A_i and H_i , namely

$$A_i = \varepsilon a_i \frac{\rho_i^v}{\langle \rho^v \rangle} \frac{\rho_i^u}{\langle \rho^u \rangle} \frac{\ell_i}{\ell_1 + \ell_2} \quad \text{and} \quad H_i = h_i \left(\frac{\rho_i^v}{\langle \rho^v \rangle} \right)^{-1} \left(\frac{\ell_i}{\ell_1 + \ell_2} \right)^{-1} .$$

355 The landscape-level functional response, $\widehat{\phi}$, has exactly the same qualitative properties as
 356 ϕ : it grows monotonically and approaches an asymptote (Figure 3). Thus, the effective

357 attack rate and handling time on the landscape-level are

$$A_{\text{eff}} = \widehat{\phi}'(0) = A_1 + A_2 \quad \text{and} \quad H_{\text{eff}} = \frac{1}{\widehat{\phi}(\infty)} = \left(\frac{1}{H_1} + \frac{1}{H_2} \right)^{-1}. \quad (19)$$

358 We can express these two quantities in terms of their habitat-level parameters and only
 359 three ratios, namely, R^u , R^ℓ , and $R^v = \rho_1^v / \rho_2^v$ as

$$A_{\text{eff}} = \varepsilon(R^\ell + 1) \frac{a_1 R^u R^v R^\ell + a_2}{(R^u R^\ell + 1)(R^v R^\ell + 1)} \quad \text{and} \quad H_{\text{eff}} = \frac{R^v R^\ell + 1}{\frac{R^v R^\ell}{h_1} + \frac{1}{h_2}}. \quad (20)$$

360 Since the landscape-level handling time, H_{eff} , is a harmonic mean with weights $R^v R^\ell$,
 361 it is monotone in R^v and R^ℓ (Figure 4(a)). The effective attack rate, however, depends
 362 strongly on how predator and prey use space relative to one another. If both spend
 363 more of their time in the same (different) habitat type, the effective attack rate increases
 364 (decreases) (Figure 4(b)).

365 The effective attack rate and handling time (19) are both averages of the scaled habitat-
 366 level attack rates and handling times. Specifically, a_i is scaled by the proportion of time
 367 the prey spend in type- i habitat ($\frac{\rho_i^u}{\langle \rho^u \rangle} \cdot \frac{\ell_i}{\ell_1 + \ell_2}$) and relative predator density in type- i habitat
 368 ($\frac{\rho_i^v}{\langle \rho^v \rangle}$). Handling time h_i is scaled by the reciprocal of relative time the predator spends
 369 in type- i habitat ($\frac{\rho_i^v}{\langle \rho^v \rangle} \cdot \frac{\ell_i}{\ell_1 + \ell_2}$).

370 Given the effective attack rate and handling time, as well as the shape of the function,
 371 it is tempting to write the landscape-level functional response as

$$\widetilde{\phi}(U) = \frac{A_{\text{eff}} U}{1 + A_{\text{eff}} H_{\text{eff}} U}. \quad (21)$$

372 However, we show that $\widetilde{\phi}(U) > \widehat{\phi}(U)$ for all $U > 0$ (Supplementary Material S.4). There-
 373 fore, while the effective landscape-level attack rate and handling time can be obtained
 374 from the habitat-level quantities through appropriate averaging, the actual functional re-
 375 sponse is always below the simple Holling type II functional response one could obtain

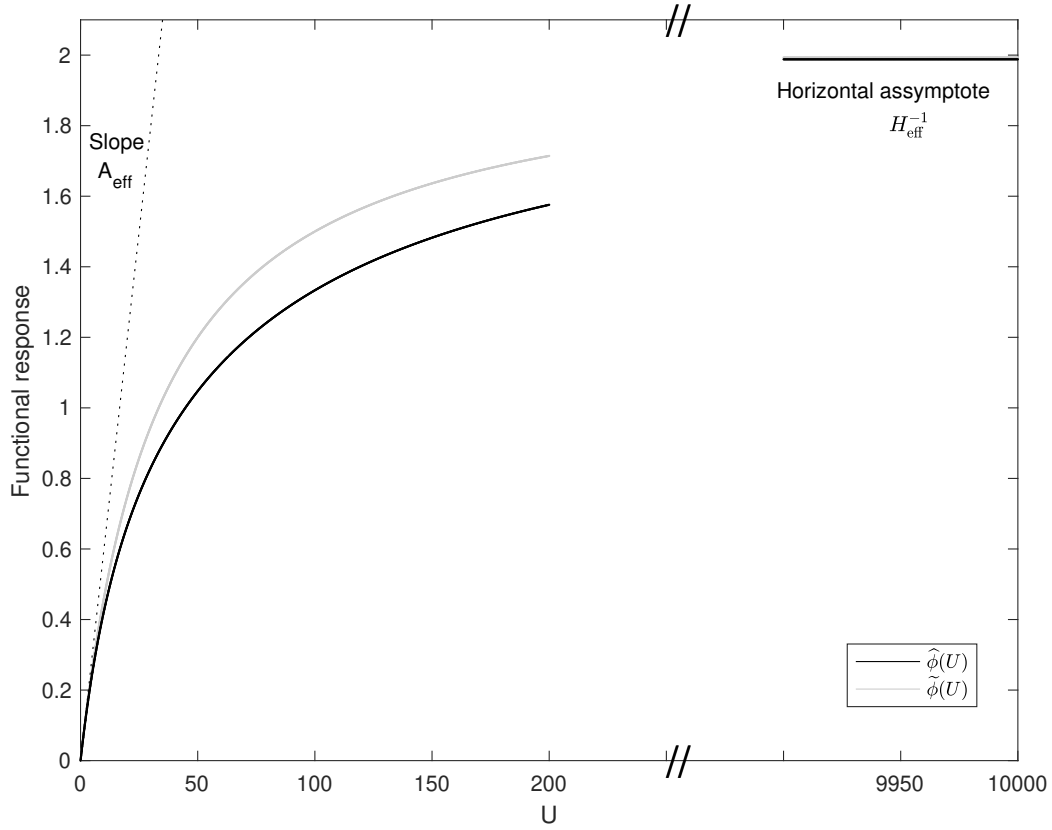


Figure 3: Landscape-level functional response ((18), black curve) and corresponding “best guess” Holling type II functional response ((21), grey curve). Both functions have slope A_{eff} at the origin (dotted line) and approach the same asymptote as U approaches infinity. The landscape-level functional response always lies below the Holling type II functional response. Parameters: $A_1 = 0.01$, $A_2 = 0.05$, $H_i = 1$.

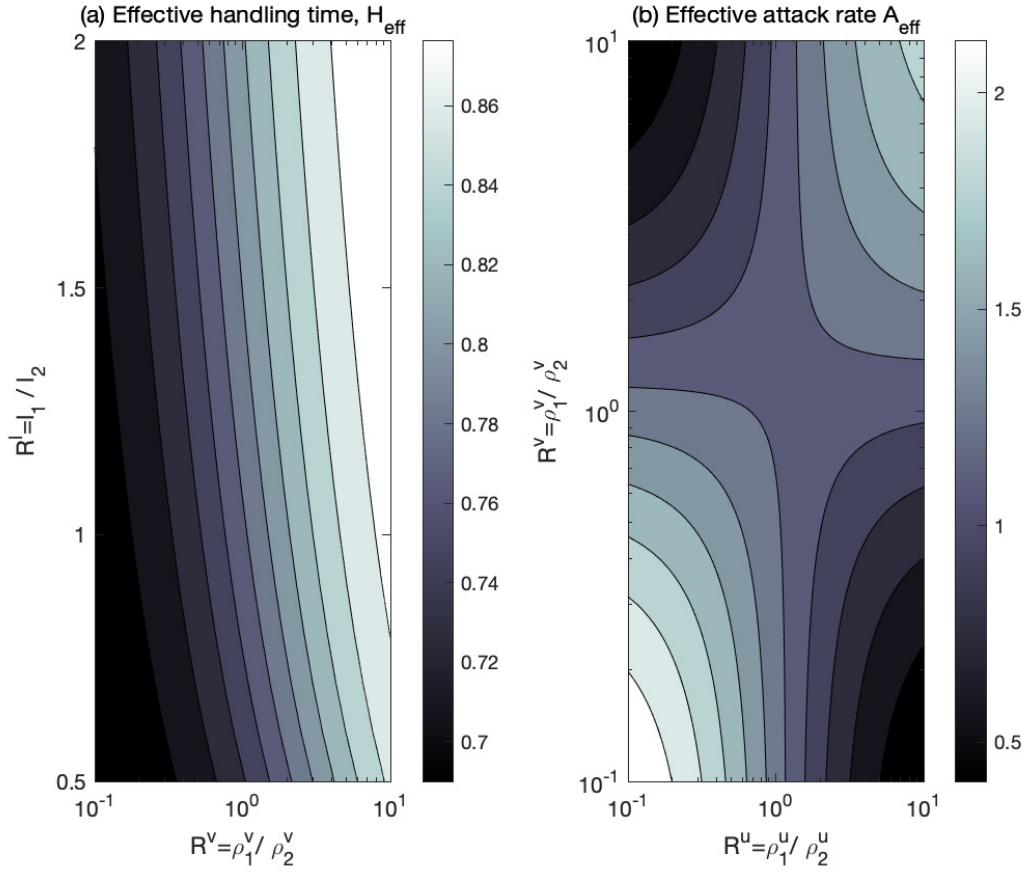


Figure 4: Effective handling time (a) and attack rate (b) as functions of the ratios of the residence indices and the patch lengths. Parameters: $a_1 = 1$, $a_2 = 1.25a_1$, $h_1 = 1$, $h_2 = 0.75h_1$, $R^\ell = 1$.

376 through assuming that (21) applies at the landscape-level. This means that one cannot
 377 get the correct landscape-level functional response by fitting (21) to aggregated data. In-
 378 stead, one has to go through the bottom-up approach described in the previous section.
 379 Using $\tilde{\phi}$ instead of $\hat{\phi}$ will overestimate the predator’s likelihood of persistence and speed
 380 of spread, as we shall see in the subsequent two sections.

381 3.3.2 Implicit spatial dynamics: predator persistence

382 The predator persists at the landscape-scale when the prey-only state, $(U^*, 0)$, is unstable,
 383 i.e., when

$$\gamma\hat{\phi}(U^*) > m. \quad (22)$$

384 This condition depends on the effects of movement behavior as expressed through the
 385 ratios of the residence indices ($R^u = \rho_1^u/\rho_2^u$ and $R^v = \rho_1^v/\rho_2^v$). The predator can persist
 386 unconditionally when the prey spends roughly equal time in both habitat types (Figure 5).
 387 When the prey spends much more time in one of the two habitats, then the predator must
 388 match that relative residence time in order to persist. However, if prey spend most of
 389 their time in habitat where prey growth rate is low (R^u small in Figure 5(a)) or negative
 390 (R^u small in 5(b)), the predator will go extinct, independent of its movement behavior.
 391 Obviously, the predator will go extinct if the prey itself cannot persist (shaded region in
 392 Figure 5(b)), but the relationship between movement behavior and predator persistence
 393 in the other cases warrants closer consideration.

394 Two mechanisms underlie our observations: the attack rate increases when the move-
 395 ment behaviors are aligned (Figure 4(b)), and there are nonlinear relationships between
 396 U^* , $\hat{\phi}(U^*)$ and R^u . Prey density at the prey-only steady state (U^*) is lowest when prey
 397 spend most of their time in poorer quality habitat and intermediate when they spend
 398 most of their time in higher quality habitat (Figure 6(a)). The maximum occurs when
 399 the time spent in the two habitats is roughly equal, so that the benefits of high growth
 400 rates balance with the cost of high intraspecific competition (Yurk and Cobbold, 2018).

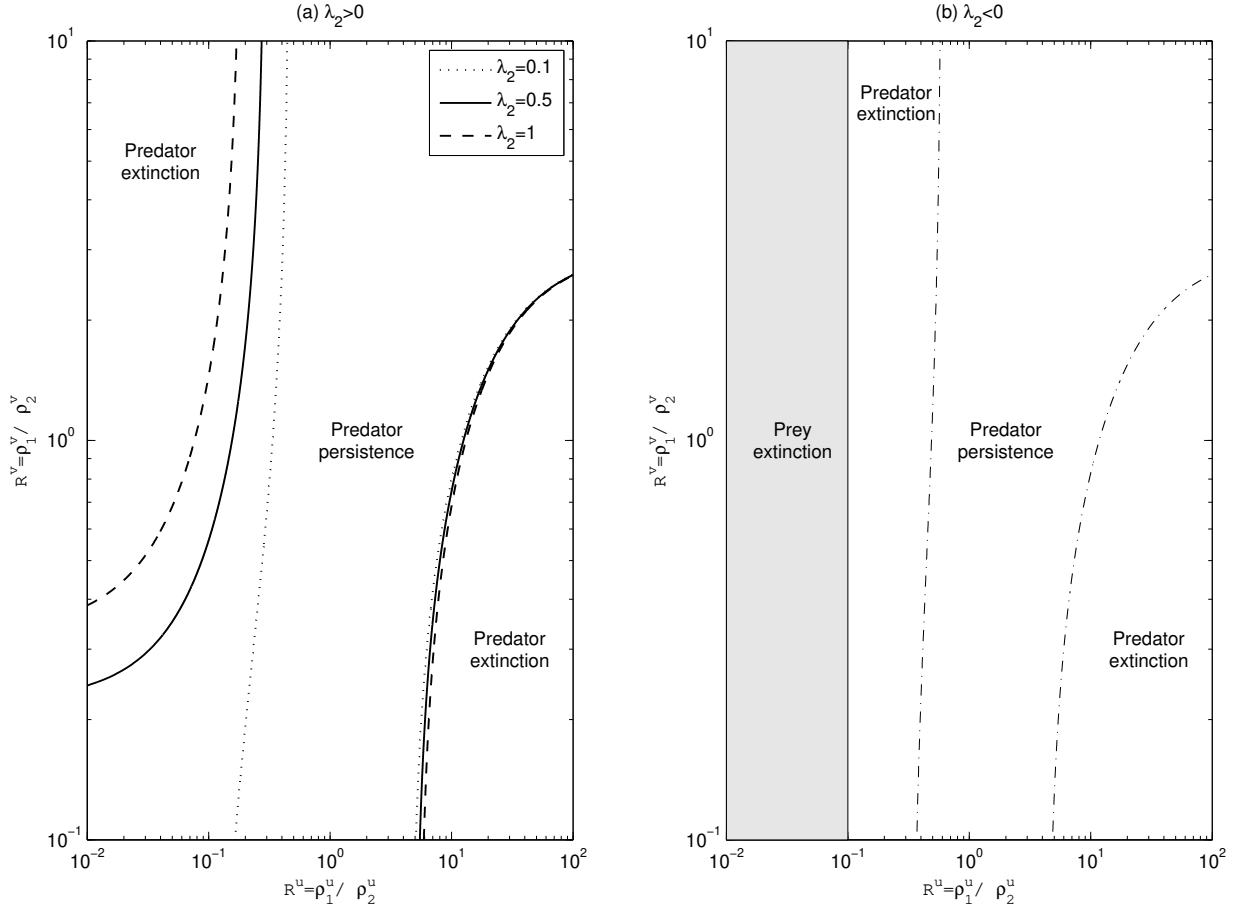


Figure 5: Predator persistence condition (22) as a function of the relative residence indices of predator and prey ($R^u = \rho_1^u / \rho_2^u$ and $R^v = \rho_1^v / \rho_2^v$). Predators persist between the pair of corresponding curves and become extinct outside this region, where predator movement behavior does not align with prey movement behavior. (a) both habitats are source habitats ($\lambda_1 \geq \lambda_2 > 0$); (b) type 2 is a sink habitat ($\lambda_1 > 0 > \lambda_2$). Parameters: $\lambda_1 = \mu_i = a_i = h_i = R^\ell = 1$, $\gamma = 5$, $m = 3.75$.

401 The relationship between R^u and $\widehat{\phi}(U^*)$ that determines predator persistence does not
 402 necessarily reflect the relationship between R^u and U^* since $\widehat{\phi}$ also depends on R^u ex-
 403 plicitly. When prey use habitats roughly equally ($R^u \approx 1$), predator growth rate is fairly
 404 insensitive to predator space use (Figure 6(b)). When prey spend more time in good
 405 habitat ($R^u \gg 1$), predator growth rate is high when predators also spend most of their
 406 time in good habitat (dotted curve). Analogously, when prey spend more time in bad
 407 habitat ($R^u \ll 1$), prey density is low but predators can still have a high growth rate by
 408 also spending most of their time in bad (for the prey) habitat (dash-dot curve). Hence,
 409 when prey use the habitat roughly equally, prey density is maximized and determines
 410 predator growth rate. When prey use the habitat unevenly, prey density decreases, and
 411 predators have to follow this uneven habitat use to increase the attack rate.

412 3.3.3 Explicit spatial dynamics: predator spread rate

413 When predators can persist, they will spread in the landscape when introduced locally.
 414 We study how their spread rate depends on movement behavior and space use, always
 415 assuming that predator and prey can stably coexist (detailed conditions in Supplementary
 416 Material S.4). The spread rate of the predator (c^v) can be obtained from the linearization
 417 of system (13) at the prey-only state $(U^*, 0)$ (Fagan *et al.*, 2002) as

$$c^v = 2\sqrt{\widehat{D}^v(\gamma\widehat{\phi}(U^*) - m)}. \quad (23)$$

418 When we fix the movement behavior of the predator, the spread rate depends on prey
 419 movement in the same way as $\widehat{\phi}(U^*)$ and can therefore be inferred from Figure 6. For
 420 example, it is a hump-shaped function of R^u and increases with λ_2 (Figure 7(a)). Since
 421 predators spend equal time in the two habitat types ($R^v = 1$, $\widehat{D}^v = 1$), the maximum
 422 spread rate for intermediate values of R^u reflects the same two mechanisms as above:
 423 (i) prey density is highest when prey use both patch types roughly equally, and (ii) the
 424 landscape-scale attack rates are highest when prey and predator have roughly the same

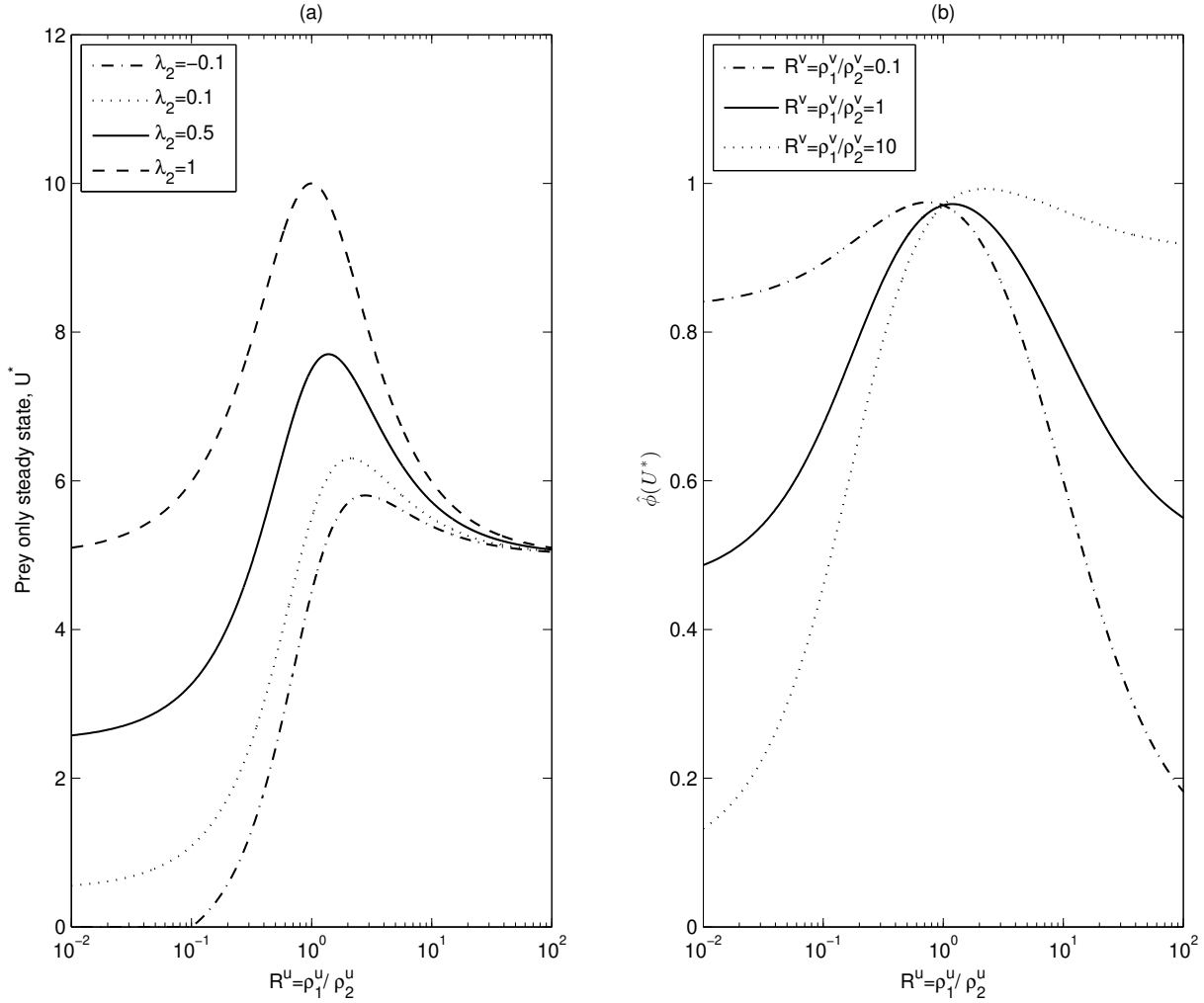


Figure 6: (a) Prey-only steady state (U^*) and (b) functional response at the prey-only steady state ($\hat{\phi}(U^*)$) as a function of the ratio of the prey residence indices $R^u = \rho_1^u / \rho_2^u$. All three scenarios in (b) correspond to the solid curve in (a). Parameters: $\lambda_1 = 1$, $\mu_i = 1$, $a_i = h_i = R^\ell = R^v = 1$ and in (b) $\lambda_2 = 0.5$.

425 ratio of residence times.

426 When predator movement behavior varies, more surprising results arise. For example,
427 increasing the predator diffusion coefficient in type-2 habitat (with all other parameters
428 fixed), does not necessarily increase predator spread rate, as we would expect. While the
429 landscape-level diffusion coefficient (5) increases with both habitat-level diffusion coeffi-
430 cients, the effective attack rate can increase *or* decrease in ρ_2^v (Figure 4) and therefore
431 also in D_2^v . Hence, while \widehat{D}^v increases with D_2^v , $\widehat{\phi}$ may increase or decrease with D_2^v . The
432 predator spread rate depends on their product (23), which can increase or decrease with
433 D_2^v . When prey spend much of their time in type-1 habitat, increasing predator movement
434 in type-2 habitat increases predator spread rate (Figure 7(b)). When prey spend very
435 little time in type-1 habitat, increasing predator movement in type-2 habitat decreases
436 predator spread rate. In the former case, prey and predator space use are increasingly
437 aligned, whereas in the latter case, they are increasingly opposed.

438 4 Discussion

439 Dispersing organisms can encounter many habitat types over the course of their lifetime.
440 Local habitat conditions and individual movement shape a population's distribution and
441 flow through the landscape. Dynamics at the landscape-scale can therefore differ signif-
442 icantly from those at the habitat-scale (Melbourne and Chesson, 2006; Thogmartin and
443 Knutson, 2007). Thus, a formal framework to systematically relate small-scale habitat-
444 level variations in conditions and behaviour to large-scale landscape-level dynamics and
445 distributions is a vital tool for deepening our understanding of the mechanisms driving
446 landscape-scale dynamics. Our HALE framework provides the desired landscape-level
447 equations, using homogenization, a technique of spatial averaging. From these landscape-
448 level equations, ecological theory can be developed that offers novel insight into how en-
449 vironmental variation shapes landscape-scale population dynamics in patchy landscapes.

450 In light of Jensen's inequality, it is not surprising that our HALE framework involves

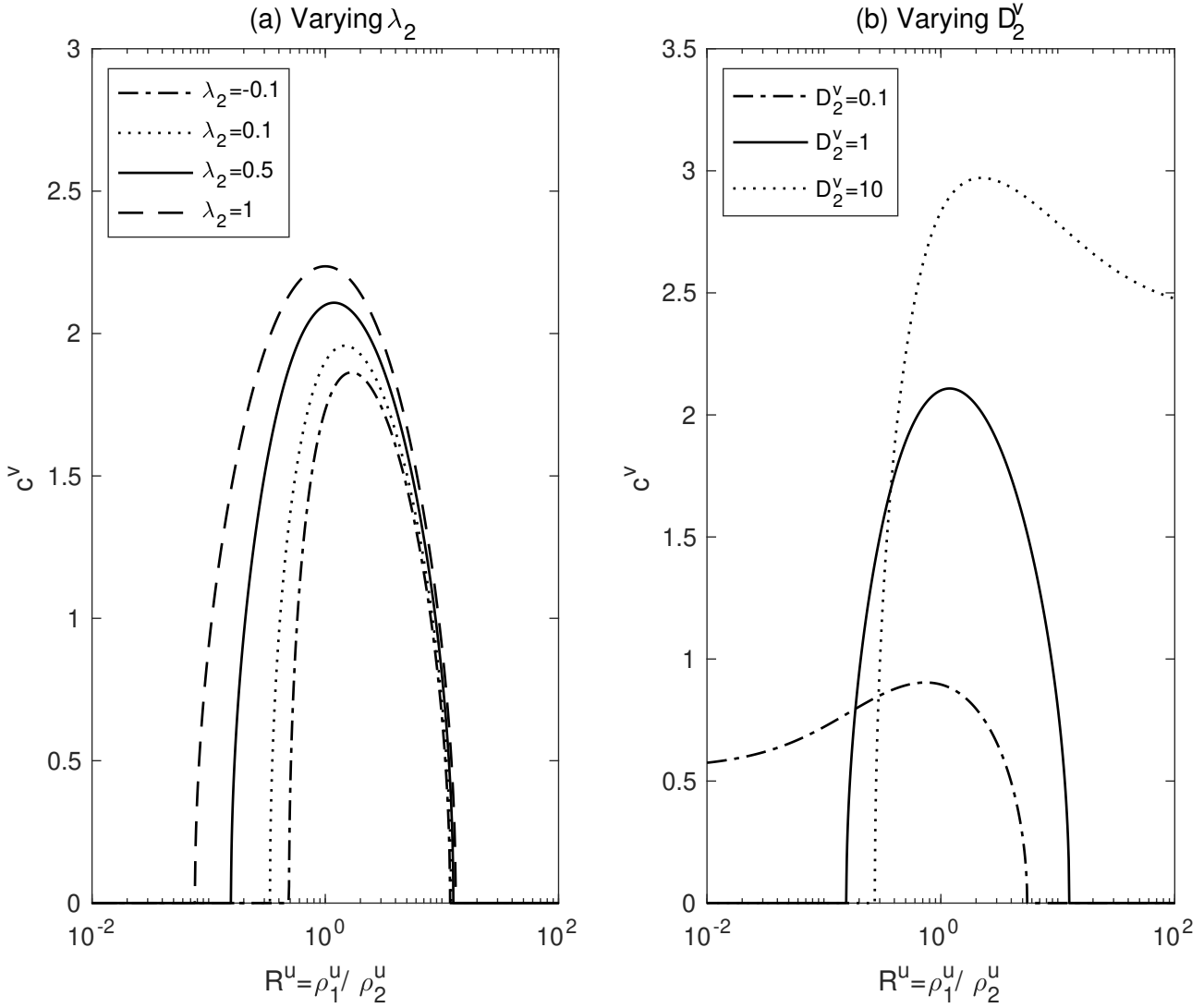


Figure 7: Predator spread rates as a function of the ratio of the prey residence indices $R^u = \rho_1^u / \rho_2^u$. We vary (a) prey low-density growth rate, and (b) predator diffusion, in habitat 2. The solid line corresponds to the same parameter set across both plots. Parameters: $\lambda_1 = 1$, $\lambda_2 = 0.5$, $\gamma = 5$, $m = 3.75$, $\mu_i = a_i = h_i = R^\ell = R^v = 1$, $\widehat{D}^v = 1$ and in (b) $D_1^v = 1$, $\alpha^v = 0.5$, giving $R^v = D_2^v$ and $\widehat{D}^v = 2R^v / (R^v + 1)$.

451 averaging the model (habitat-level growth and interaction functions) rather than the
452 data (habitat-level parameters). It has been widely recognized that one cannot simply
453 average environmental conditions to infer dynamics (Ruel and Ayres, 1999). Non-linear
454 response functions together with environmental variance can shift the dynamical behavior
455 away from what linearly averaged conditions would predict. This observation is also at
456 the heart of *scale transition theory* (Melbourne and Chesson, 2006; Chesson, 2012), an
457 alternative framework for scaling from habitat to landscape-level models.

458 As with our approach, scale transition theory may also begin with a high-resolution
459 patch model (e.g., equations (2)) that explicitly incorporates individual movement, organ-
460 isms' habitat choices, and heterogeneity. The high-resolution patch model can be solved
461 to predict spatial covariances between the densities of interacting species or between pop-
462 ulation densities and local landscape characteristics that affect fitness (Chesson, 2012).
463 Scale transition theory accounts for these covariances in approximating landscape-level
464 quantities that emerge as parameters in dynamical models of spatially averaged popula-
465 tion densities. At the heart of both approaches is the assumption that dispersal processes
466 occur at a faster rate than demographic processes so that local variation in relative pop-
467 ulation densities is determined largely by habitat-level movement rates.

468 Our work differs from scale transition theory and other existing up-scaling methods
469 (Metz, 2000; Morozov and Poggiale, 2012) in that the result is a landscape-level model
470 that remains spatially explicit. While other methods average out spatial variation across
471 the entire landscape, including for the state variables, the HALE framework averages out
472 habitat-level but not landscape-level variation. Spatial resolution is reduced, simplifying
473 the model, but not lost altogether. Our approach retains the influence of local variation
474 in habitat type, habitat quantity, and species movement rules, and reveals how these rules
475 change as we move from habitat to landscape-scale. Most notably, we retain the ability
476 to predict their effects on large-scale spatio-temporal dynamics, e.g., invasion speeds.

477 The importance and insights of a bottom-up approach are illustrated by our predator–

478 prey example in section 3.3. Predator attack rate at the landscape-scale is maximized
479 when prey and predator align their space use so that their ratios of the habitat residence
480 times are similar ($R^u \approx R^v$). Aligning space use might seem a surprising strategy when it
481 requires a predator to have a high residence time where habitat-level attack rates are low
482 (Figure 5(b), top right). The landscape-level attack rate is high because predators spend
483 most of their time in the same locations as the prey. Even though attacks may be less
484 successful in these locations, the number of encounters keeps the landscape-level attack
485 rate high. Essentially, there is little benefit to being efficient at catching prey in locations
486 where prey rarely go (Figure 5(b), bottom right). When habitats are “spatial anchors”
487 for both prey and predator then their space use has been shown to align (Smith *et al.*,
488 2019). In the puma-vincuña system in Argentina, predators preferred meadow habitat
489 as it provided cover when stalking prey, while prey relied on meadow habitat for foraging,
490 despite the increased predation risk. Aligning space use ultimately favored the predators,
491 as they successfully found and killed their prey, a result predicted by our landscape-scale
492 attack rates.

493 Since our HALE framework is based on residence indices, it easily accommodates
494 recent advances in inference and statistical modeling of spatial movement. For exam-
495 ple, Hooten *et al.* (2019) provide a method for estimating residence times using resource
496 selection functions and partial differential equations. They capitalize on the growing avail-
497 ability of spatial movement data from telemetry tracking and aerial surveys. Telemetry
498 data can be used to estimate residence times at the habitat scale even when this scale is
499 small (e.g. meters). For example, Johnson *et al.* (2008) developed methods to extrapo-
500 late paths between GPS measurements, which Garlick *et al.* (2011) successfully used to
501 calculate residence times for mule deer on 30m \times 30m grid squares, the typical scale of
502 land cover maps.

503 Our approach also provides a mathematically sound method for dealing with issue of
504 biases that are introduced when scaling up landscape maps for use in dynamic modeling.

505 Bocedi *et al.* (2012) assessed how range expansion is affected by the resolution of the
506 landscape, dispersal and demography in dynamic simulation models. Such models are
507 increasingly used to make predictions about potential impacts of climate change and land
508 management. Often, grid cells from raster maps are aggregated to facilitate computation
509 over large geographical areas, but this aggregation is typically done in a naïve way, without
510 considering, for example, that the upscaled mean dispersal distance or prey handling time
511 on a larger grid cell may not be spatial averages of those on the finer resolution grid.
512 Bocedi *et al.* (2012) found that the extent of range expansion was overestimated when
513 landscape maps and ecological processes were upscaled using simple spatial averages. We
514 make the same prediction for predator invasion speeds (see section 3.3.1), but are also
515 able to attribute mechanism to this behaviour. Overestimation can arise if one assumes
516 that the ecological process (here predator functional response) in the upscaled model
517 has the same functional form as in the fine-scale model. This assumption is invalid
518 because of the interaction between nonlinearity in the functional response and spatial
519 variation (Chesson, 2012). We provide a method for correctly scaling up these ecological
520 processes and removing the systematic biases that can occur when upscaling is done in a
521 naïve way. Homogenization, the foundation of our method, accurately predicts upscaled
522 dispersal kernels and rates of range expansion (Garlick *et al.*, 2011; Yurk and Cobbold,
523 2018; Duncan *et al.*, 2017).

524 Our idealized landscape consists of two periodically alternating habitat types. Our
525 method generalizes to multiple habitat types by replacing the averages in equation (4)
526 with their multi-type equivalences (Supplementary Material S.1). Individuals still need to
527 encounter these habitats many times over their lifetime, i.e., patches must be small. Such
528 a requirement is reasonable. For example, mule deer explore up to 38 habitat (land cover)
529 types during a season in southern Utah (Garlick *et al.*, 2014), so that the requirements
530 of the theory are easily satisfied. Our approach also generalizes to more than two species
531 (Garlick *et al.*, 2014).

532 It is more challenging to generalize the method to non-periodic landscapes. In fact, if
533 landscape composition changes fundamentally over the scale of interest, one cannot expect
534 a landscape-scale equation with spatially constant coefficients to accurately represent the
535 dynamics of populations. Homogenization theory, however, does not require periodicity. If
536 habitat types vary on a small *and* on a larger scale, homogenization theory can be used to
537 derive large-scale equations that contain spatially changing small-scale averages (Pavliotis
538 and Stuart, 2008). The resulting equations are still difficult to analyze, but there is
539 a highly relevant intermediate case. Landscapes are often quasi-periodic, i.e., there is
540 a spatial scale, larger than the habitat-scale, at which the habitat-level averages are
541 relatively constant. For example, landscapes in southern Utah are reasonably close to
542 quasi-periodic (Garlick *et al.*, 2011). In that case, one can apply homogenization for
543 periodic landscapes, but the mathematical derivation of this result is more cumbersome.

544 Our method is formulated for one-dimensional landscapes. While such a simplification
545 is reasonable when studying spatial spread, other applications require two-dimensional
546 models. The formulation of reaction-diffusion equations in two-dimensional homogeneous
547 landscapes is straight forward (Turchin, 1998), and corresponding matching conditions at
548 interfaces between habitat types have also been derived (Ovaskainen and Cornell, 2003).
549 Applying homogenization theory is much harder in two dimensions. Garlick *et al.* (2014)
550 gave mathematical formulas for the case of an ecological diffusion operator even in an
551 aperiodic landscape, but without preference for certain habitat types. Habitat preference
552 can induce directionality in overall movement behavior that makes homogenization diffi-
553 cult. In the one-dimensional case that we presented, it is relatively easy to ensure that
554 this directionality averages to zero at the landscape scale, i.e., even though individuals
555 prefer one patch type over another locally, their movement shows no preferred direction
556 on the landscape scale. Our results are expressed not only in mathematical formulas but
557 in certain averages of ecologically relevant and measurable quantities, which are in some
558 sense “coordinate free”. In fact, quantities such as the average residence time can be

559 measured for two-dimensional landscapes and then be used in our formulas even if some
560 local information is not available separately.

561 HALE provides a comprehensive framework for scaling up spatially explicit models for
562 diffusive movement of organisms in small-scale patchy environments to give landscape-
563 scale descriptions of population dynamics. Various aspects of the theory underlying
564 our approach have previously been used to successfully study the spread of wildlife dis-
565 eases (Garlick *et al.*, 2014), insects (Powell and Bentz, 2014) and plants (Powell and
566 Zimmermann, 2004). These studies focused on the movement processes only and in the
567 absence of edge-related behavior. Our approach encompasses those applications and il-
568 lustrates how we can scale up ecological processes in a systematic and informative way
569 that connects to classical concepts in ecology, namely residence index and dynamic level.
570 From the HALE framework we can develop ecological theory to explain the contrasting
571 dynamics that can sometimes be observed between habitat- and landscape-scale studies.
572 At the heart of our findings is the insight that fine-scale movement and behavior can have
573 marked effects on landscape-level outcomes through the interaction of nonlinear response
574 functions and environmental variation.

575 **Acknowledgments**

576 This work was supported by the American Institute of Mathematics SQuaREs program.
577 The authors gratefully thank James Powell, Marti Garlick, and Thomas Hillen for many
578 helpful discussions that shaped and inspired this paper. Part of this work was carried out
579 while CC visited FL supported by the University of Ottawa Visiting Researchers Program.
580 It was completed while CC was supported by a Leverhulme Research Fellowship RF-2018-
581 577\9. FL is supported by the Natural Sciences and Engineering Research Council of
582 Canada (RGPIN-2016-04795 and RGPAS-2016-492872). BY was supported by a Jacob
583 E. Nyenhuis Faculty Development Grant from Hope College.

584 **Statement of contributions**

585 BY, CAC, FL conceived the ideas and BY designed method; CAC conducted the numerical
586 work; CAC and FL led the writing of the manuscript. All authors contributed critically
587 to the drafts and gave final approval for publication.

588 **References**

589 Alqawasmeh, Y. and Lutscher, F. (2019). Persistence and spread of stage-structured pop-
590 ulations in heterogeneous landscapes. *Journal of Mathematical Biology*, **78**(5), 1485–
591 1527.

592 Bergström, U., Englund, G., and Leonardsson, K. (2006). Plugging space into predator-
593 prey models an empirical approach. *The American Naturalist*, **167**, 246–259.

594 Bocedi, G., Pe'er, G., Heikkinen, R., Matsinos, Y., and Travis, J. J. (2012). Project-
595 ing species' range expansion dynamics: sources of systematic biases when scaling up
596 patterns and processes. *Methods in Ecology and Evolution*, **3**, 1008–018.

597 Chesson, P. (1998). Making sense of spatial models in ecology. *Modeling spatiotemporal*
598 *dynamics in ecology*, pages 151–166.

599 Chesson, P. (2012). Scale transition theory: Its aims, motivations and predictions. *Eco-*
600 *logical Complexity*, **10**, 52–68.

601 Chesson, P., Donahue, M., Melbourne, B., and Sears, A. (2005). Scale transition the-
602 ory for understanding mechanisms in metacommunities. In M. Holyoak, M. Leibold,
603 and R. Holt, editors, *Meta-communities: Spatial dynamics and ecological communities*.
604 University of Chicago Press, Chicago.

605 Crone, E. and Schultz, C. (2008). Old models explain new observations of butterfly
606 movement at patch edges. *Ecology*, **89**(7), 2061–2067.

607 Crone, E., Brown, L., Hodgson, J., Lutscher, F., and Schultz, C. (2019). Faster movement
608 in habitat matrix promotes range shifts in heterogeneous landscapes. *Ecology*, **100**(7),
609 e02701.

610 Duncan, J., Rozum, R., Powell, J., and Kettenring, K. (2017). Multi-scale methods
611 predict invasion speeds in variable landscapes. *Theoretical Ecology*, **10**(3), 287–303.

612 Englund, G. and Cooper, S. (2003). Scale effects and extrapolation in ecological experi-
613 ments. In C. Caswell, editor, *Advances in ecological research*. Associated Press.

614 Englund, G. and Leonardsson, K. (2008). Scaling up the functional response for spatially
615 heterogeneous systems. *Ecology Letters*, **11**, 440–449.

616 Fagan, W., Lewis, M., Neubert, M., and van den Driessche, P. (2002). Invasion theory
617 and biological control. *Ecology Letters*, **5**, 148–157.

618 Garlick, M., Powell, J., Hooten, M., and MacFarlane, L. (2011). Homogenization of large-
619 scale movement models in ecology. *Bulletin of Mathematical Biology*, **73**, 2088–2108.

620 Garlick, M., Powell, J., Hooten, M., and MacFarlane, L. (2014). Homogenization, sex, and
621 differential motility predict spread of chronic wasting disease in mule deer in southern
622 Utah. *Journal of Mathematical Biology*, **69**(2), 369–399.

623 Getz, W. M., Marshall, C. R., Carlson, C. J., Giuggioli, L., Ryan, S. J., Romañach, S. S.,
624 Boettiger, C., Chamberlain, S. D., Larsen, L., D’Odorico, P., *et al.* (2018). Making
625 ecological models adequate. *Ecology letters*, **21**(2), 153–166.

626 Gilbert, M., White, S., Bullock, J., and Gaffney, E. (2017). Speeding up the simulation
627 of population spread models. *Methods in Ecology and Evolution*, **8**, 501–510.

628 Hastings, A. (2012). Temporally varying resources amplify the importance of resource
629 input in ecological populations. *Biology Letters*, **8**, 1067–1069.

- 630 Hewitt, J., Thrush, S., Dayton, P., and Bonsdorff, E. (2007). The effect of spatial and tem-
631 poral heterogeneity on the design and analysis of empirical studies of scale-dependent
632 systems. *The American Naturalist*, **169**(3), 398–408.
- 633 Hooten, M., Lu, X., Garlick, M., and Powell, J. (2019). Animal movement models with
634 mechanistic selection functions. *Spatial Statistics*, **37**, 100406.
- 635 Inouye, B. (2005). Scaling up from local competition to regional coexistence across two
636 scales of spatial heterogeneity: insect larvae in the fruits of *Apeiba membranacea*. *Oe-*
637 *cologia*, **145**(2), 187–195.
- 638 Johnson, D., London, J., Lea, M., and Durban, J. (2008). Continuous-time correlated
639 random walk model for animal telemetry data. *Ecology*, **89**, 1208–1215.
- 640 Lutscher, F. and Hillen, T. (2021). Correlated random walks in heterogeneous landscapes:
641 derivation, homogenization and population spread rates. *AIMS Mathematics* *6*(8):,
642 **6**(8), 8920–8948.
- 643 Lutscher, F. and Musgrave, J. (2017). Behavioral responses to resource heterogeneity can
644 accelerate biological invasions. *Ecology*, **98**(5), 1229–1238.
- 645 Maciel, G. and Lutscher, F. (2013). How individual response to habitat edges affects
646 population persistence and spatial spread. *The American Naturalist*, **182**(1), 42–52.
- 647 Maciel, G. and Lutscher, F. (2018). Movement behavior determines competitive outcome
648 and spread rates in strongly heterogeneous landscapes. *Theoretical Ecology*, **11**(3),
649 351–365.
- 650 Melbourne, B. and Chesson, P. (2006). The scale transition: scaling up population dy-
651 namics with field data. *Ecology*, **87**(6), 1478–1488.
- 652 Metz, H. (2000). *The geometry of ecological interactions: simplifying spatial complexity*.
653 Cambridge University Press.

654 Morozov, A. and Poggiale, J.-C. (2012). From spatially explicit ecological models to
655 mean-field dynamics: The state of the art and perspectives. *Ecological Complexity*, **10**,
656 1–11.

657 Neupane, R. and Powell, J. (2015). Invasion speeds with active dispersers in highly variable
658 landscapes: Multiple scales, homogenization, and the migration of trees. *Journal of*
659 *Theoretical Biology*, **387**, 111–119.

660 Ovaskainen, O. and Cornell, S. (2003). Biased movement at a boundary and conditional
661 occupancy times for diffusion processes. *Journal of Applied Probability*, **40**(3), 557–580.

662 Painter, J. and Hillen, T. (2015). Navigating the flow: individual and continuum mod-
663 els for homing in flowing environments. *Journal of the Royal Society Interface*, **12**,
664 20150647.

665 Pavliotis, G. and Stuart, A. (2008). *Multiscale Methods: Averaging and Homogenization*.
666 Springer, New York.

667 Powell, J. and Bentz, B. (2014). Phenology and density-dependent dispersal predict pat-
668 terns of mountain pine beetle (*Dendroctonus ponderosae*) impact. *Ecological Modelling*,
669 **273**, 173–185.

670 Powell, J. and Zimmermann, N. (2004). Multiscale analysis of active seed dispersal con-
671 tributed to resolving Reid’s paradox. *Ecology*, **85**(2), 490–506.

672 Reeve, J., Cronin, J., and Haynes, K. (2008). Diffusion models for animals in complex
673 landscapes: incorporating heterogeneity among substrates, individuals and edge be-
674 haviours. *Journal of Animal Ecology*, **77**, 898–904.

675 Ruel, J. and Ayres, M. (1999). Jensen’s inequality predicts effects of environmental
676 variation. *Trends in Ecology and Evolution*, **14**(9), 361–366.

- 677 Shigesada, N., Kawasaki, K., and Teramoto, E. (1986). Traveling periodic waves in
678 heterogeneous environments. *Theoretical Population Biology*, **30**, 143–160.
- 679 Skellam, J. (1973). The formulation and interpretation of mathematical models of dif-
680 fusional process in population biology. In M. Bartlett and R. Hiorns, editors, *The*
681 *mathematical theory of the dynamic of biological populations*, pages 63–85. Academic
682 Press, London.
- 683 Smith, J., Donadio, E., Pauli, J., Sheriff, M., Bidder, O., and A.D., M. (2019). Habitat
684 complexity mediates the predator-prey space race. *Ecology*, **100**(7), e02724.
- 685 Thogmartin, W. and Knutson, M. (2007). Scaling local species-habitat relations to the
686 larger landscape with a hierarchical spatial count model. *Landscape Ecology*, **22**, 61–77.
- 687 Turchin, P. (1998). *Quantitative Analysis of Movement: measuring and modeling popula-*
688 *tion redistribution of plants and animals*. Sinauer Associates, Sunderland, MA.
- 689 Wheatley, M. and Johnson, C. (2009). Factors limiting our understanding of ecological
690 scale. *Ecological complexity*, **6**(2), 150–159.
- 691 Yurk, B. and Cobbold, C. (2018). Homogenization techniques for population dynamics
692 in strongly heterogeneous landscapes. *Journal of Biological Dynamics*, **12**, 171–193.